A new probabilistic seismic hazard assessment for greater Tokyo

BY ROSS S. STEIN[1,*], SHINJI TODA[2], TOM PARSONS[1]
AND ELLIOT GRUNEWALD[1,3]

[1]*US Geological Survey, Menlo Park, CA 94025, USA*
[2]*Active Fault Research Center, AIST, Tsukuba 305-8567, Japan*
[3]*Department of Geophysics, Stanford University, Stanford,
CA 94305-2215, USA*

Tokyo and its outlying cities are home to one-quarter of Japan's 127 million people. Highly destructive earthquakes struck the capital in 1703, 1855 and 1923, the last of which took 105 000 lives. Fuelled by greater Tokyo's rich seismological record, but challenged by its magnificent complexity, our joint Japanese–US group carried out a new study of the capital's earthquake hazards. We used the prehistoric record of great earthquakes preserved by uplifted marine terraces and tsunami deposits (17 $M \sim 8$ shocks in the past 7000 years), a newly digitized dataset of historical shaking (10 000 observations in the past 400 years), the dense modern seismic network (300 000 earthquakes in the past 30 years), and Japan's GeoNet array (150 GPS vectors in the past 10 years) to reinterpret the tectonic structure, identify active faults and their slip rates and estimate their earthquake frequency. We propose that a dislodged fragment of the Pacific plate is jammed between the Pacific, Philippine Sea and Eurasian plates beneath the Kanto plain on which Tokyo sits. We suggest that the Kanto fragment controls much of Tokyo's seismic behaviour for large earthquakes, including the damaging 1855 $M \sim 7.3$ Ansei-Edo shock. On the basis of the frequency of earthquakes beneath greater Tokyo, events with magnitude and location similar to the $M \sim 7.3$ Ansei-Edo event have a *ca* 20% likelihood in an average 30 year period. In contrast, our renewal (time-dependent) probability for the great $M \geq 7.9$ plate boundary shocks such as struck in 1923 and 1703 is 0.5% for the next 30 years, with a time-averaged 30 year probability of *ca* 10%. The resulting net likelihood for severe shaking (*ca* 0.9*g* peak ground acceleration (PGA)) in Tokyo, Kawasaki and Yokohama for the next 30 years is *ca* 30%. The long historical record in Kanto also affords a rare opportunity to calculate the probability of shaking in an alternative manner exclusively from intensity observations. This approach permits robust estimates for the spatial distribution of expected shaking, even for sites with few observations. The resulting probability of severe shaking is *ca* 35% in Tokyo, Kawasaki and Yokohama and *ca* 10% in Chiba for an average 30 year period, in good agreement with our independent estimate, and thus bolstering our view that Tokyo's hazard looms large. Given $1 trillion estimates for the cost of an $M \sim 7.3$ shock beneath Tokyo, our probability implies a $13 billion annual probable loss.

Keywords: Ansei-Edo; Kanto; Genroku; Yokohama; Kawasaki; Boso

1. Introduction

The Japanese government recently issued a report furnishing a probabilistic hazard assessment for large earthquakes on the plate boundary megathrusts and the 98 most active faults in Japan and their associated shaking (Earthquake Research Committee 2005). Our Japan–US team sought to probe more deeply into the areas of greatest uncertainty identified by the government study, developing new datasets and analytical methods, and pursuing new means to corroborate our derived probabilities. We relied on observational evidence rather than models of seismic behaviour wherever possible, focusing greatest attention on the likelihood of earthquakes capable of producing severe shaking (Japan Meteorological Agency (JMA) Intensity 6, equivalent to a PGA of $ca\,0.9g$; Karim & Yamazaki 2002) in the highly populated Tokyo–Yokohama corridor and the southern Kanto plain. Here, we summarize our broad approach and conclusions.

2. Kanto plate tectonic configuration

Three of the Earth's tectonic plates meet 300 km east of Tokyo, and a chain of active volcanoes lies just 100 km to the west (figure 1a). To understand the geometry of this so-called 'triple junction' and identify the faults on which large earthquakes can strike, we examined 320 000 microearthquakes in a three-dimensional geographic information system and used 6000 of these to carry out a seismic tomographic inversion (Toda et al. submitted). On the basis of the microearthquake distributions, seismic tomography and seismic stress inversion, we propose that a 90×120 km wide dislodged fragment of the Pacific plate is wedged beneath Tokyo between the Pacific, Philippine Sea and Eurasian plates (figure 1b). The fragment was probably dislodged when two seamount chains collided at the Japan Trench about 2 Myr ago. We suggest that the fragment controls much of Tokyo's seismic behaviour, with the concentration of $M \leq 7.4$ shocks beneath Tokyo attributable to the sliding of the fragment against the three other plates. Unlike previous interpretations, in which the Philippine Sea plate was thought to extend 100 km north of Tokyo and reach to a depth of 90 km (Ishida 1992; Noguchi 1998), we argue that the Philippine Sea slab extends to a depth of only 35 km. If so, the leading edge of the Philippine Sea slab, and thus the northward limit of great underthrust earthquakes, extends only as far north as Tokyo (figure 1b). This interpretation differs from the prevailing view, in which all of the seismicity beneath Tokyo is attributed to the Philippine Sea plate warped and folded against the Pacific plate (Ishida 1992, 1995). The analogous bend in the Japan trench between the Japanese islands of Honshu and Hokkaido also is associated with the collision of a seamount chain, leading to a severely bent Pacific plate slab (Niu et al. 2005) and concentrated inland seismicity beneath the Hidaka basin. Unlike Kanto basin, the Hidaka basin is not associated with a triple junction, and so we regard the seismic features of the Kanto region to be principally related to the Pacific Plate, rather than to the Philippine Sea plate.
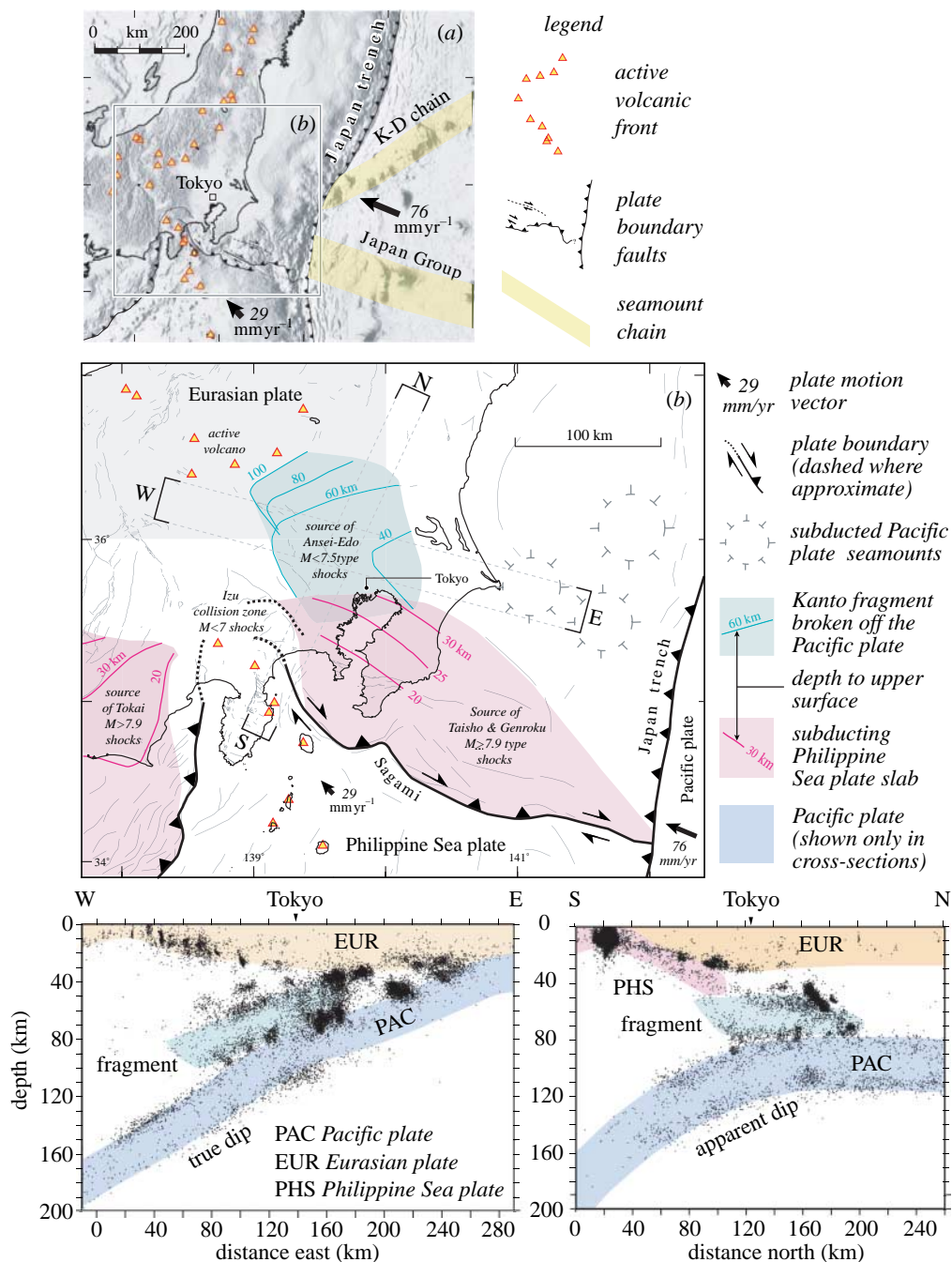
Figure 1. (*a*) Simplified tectonic map of the Kanto triple junction (Toda *et al.* submitted), showing the Japan Group and Kashima-Daiichi seamount chains. (*b*) The Philippine Sea plate is shaded pink, where it descends beneath the Eurasian plate. The proposed Kanto fragment (green) lies between the Philippine Sea plate and the underlying Pacific plate. Sites of large historical earthquakes are identified with their tectonic plate element. Two cross-sections through greater Tokyo are shown with 1979–2003 microseismicity in the lower panels.

Table 1. JMA intensity scale and equivalent ground motion parameters.

observations used to assess shaking intensity	JMA intensity scale	estimated peak ground acceleration at 5–8 Hz (g)	estimated peak ground velocity at 5–8 Hz (m s^{-1})	modified Mercalli intensity, MMI
felt by most people in the building. Some people are frightened	3	~0.02	~0.02	V
many people are frightened. Some people try to escape from danger. Most sleeping people awaken	4	~0.07	~0.07	VI
occasionally, less earthquake-resistant houses suffer damage to walls and pillars	5 lower	~0.26	~0.26	VII and VIII
occasionally, less earthquake-resistant houses suffer heavy damage to walls and pillars, and lean	5 upper			
occasionally, less earthquake-resistant houses collapse and even walls and pillars of highly earthquake-resistant houses are damaged	6 lower	~0.95	~0.93	IX and X
many less earthquake-resistant houses collapse. In some cases, even walls and pillars of highly earthquake-resistant houses are heavily damaged	6 upper			
occasionally, even highly earthquake-resistant houses are severely damaged and lean	7	~3.4	~3.3	XI and XII
source: Japan Meteorological Agency (2004)		Karim & Yamazaki (2002)		

3. Historical earthquake intensities

Compilations of earthquake shaking during 1600–1884 (Usami 1994, 2003), 1884–1923 (Utsu 1979, 1982) and 1923 (Takemura 2003; Hamada *et al.* 2001) were combined with post-1923 data through 2003 (Japan Meteorological Agency 2004), to produce a new digital database of 10 000 intensity observations for the Kanto region (Bozkurt *et al.* submitted). Intensity is generally based on written observations of shaking (table 1), and so can be used to assess earthquakes that precede the development of seismic instrumentation. The peak intensity observed within 2000 5×5 km cells during the past 400 years is shown in figure 2a. For cells containing observations for the three largest earthquakes to occur in the Kanto region during this period, similar and severe (JMA Intensity≥6) shaking intensity is seen (figure 2b–d).

These observations indicate that the 1703, 1855 and 1923 earthquakes were large, and also indicate that unconsolidated stream deposits in the Kanto plain and young sediments along the western margin of Tokyo Bay amplify the shaking.

4. Size, geometry and location of the three largest earthquakes

(a) 1 September 1923 Kanto earthquake

To evaluate the release of accumulated plate motion in the Kanto region, we reassessed the 1923 earthquake fault geometry and slip (Nyst *et al.* in press). The model provides a best fit to a new geodetic dataset consisting of vertical displacements from levelling and angle changes from triangulation measurements obtained in surveys between 1883 and 1927. We used 10 times more triangulation data than were previously available, and also corrected the observations to remove interseismic deformation (the steady deformation that occurs during the centuries between earthquakes, that is roughly opposite in sign to the coseismic motions). The location, depth and dip of the fault planes is adopted from a recent seismic reflection study of the Kanto region (Sato *et al.* 2005). The fault model consists of two adjacent 20°-dipping low-angle planes accommodating oblique reverse right-lateral slip of 6.0 m on the larger eastern plane and 9.5 m on the smaller western plane (Nyst *et al.* in press; figure 3*a*). Two sites of high slip are identified, one at the west end of the fault near the epicentre, the other beneath the mouth of Tokyo Bay (Pollitz *et al.* 2005, 2006). Most of the aftershocks of the 1923 earthquake occurred in regions where we calculate that stress transferred by the earthquake brought nearby faults closer to failure (red zones 1–2 in figure 3*a*).

(b) 11 November 1855 M∼ 7.3 Ansei-Edo earthquake

On the basis of intensity observations and reported aftershock activity, Bakun (2005) estimated $M = 7.2$ ($6.9 \leq M \leq 7.5$ at 95% confidence), an epicentre at the north margin of Tokyo Bay, and a depth between 30 and 70 km. By excluding less reliable JMA Intensity 3 (felt) observations, Grunewald (submitted) concluded that the event was $M = 7.4$, with an epicentre near Chiba (figures 2*c* and 4*a*). A nearly identical distribution of intensities was observed for the 23 July 2005 $M = 6.0$ earthquake at 70 km depth beneath Chiba, suggesting that the Ansei-Edo event might also lie at the same depth, corresponding to the North Tokyo Bay seismic cluster at the contact between the proposed Kanto fragment and the Pacific Plate (Toda *et al.* submitted; figures 3*b* and 1). The northern Tokyo Bay and southern Kanto Plain have been the site of four $M \geq 7$ shocks since 1649 (figure 4*a*), although no such earthquakes have struck since 1923. This seismic hiatus may have occurred because stress on the fault that ruptured in 1855 was subjected to a stress decrease by the 1923 Kanto earthquake (Nyst *et al.* submitted), inhibiting failure (figure 3*a*).

(c) 31 December 1703 M∼ 8.2 Genroku earthquake

Using earthquake intensity data (figure 2*d*), shorelines uplifted and deformed by the 1703 earthquake (Shishikura 2003), a newly augmented tsunami run-up height dataset, and intensity data (Grunewald submitted), we propose that the 1703 earthquake ruptured the Sagami trough fault segment at the mouth of Tokyo Bay
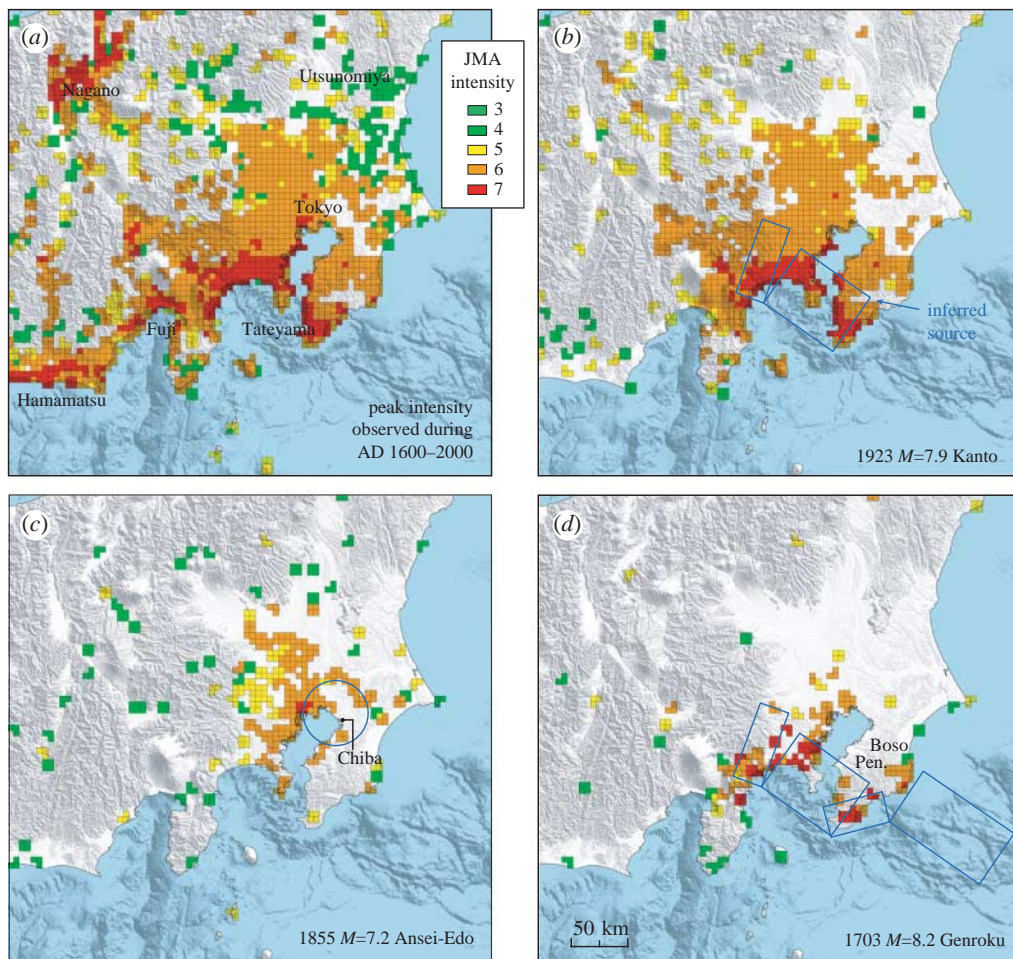
Figure 2. (*a*) Peak intensities observed during the past 400 years. Observed intensity distribution for (*b*) 1923 $M=7.9$ Kanto (*c*) 1855 $M\sim7.4$ Ansei-Edo and (*d*) 1703 $M\sim8.2$ Genroku shocks (Bozkurt *et al.* submitted), together with our inferred seismic sources for these three earthquakes.

(fault A in figure 5*a*), plus one or two segments located east of the Boso peninsula (faults B and C in figure 5*a*), resulting in a magnitude of $M\sim8.2$ (Shishikura *et al.* in preparation). Slip of the same amount also occurred in 1923 (figure 3*a*). Slip on fault B is needed to explain why the uplift of the eastern Boso peninsula was much greater in 1703 than in 1923 and fault C is needed to explain why the 1703 shock was accompanied by a substantial tsunami on the eastern Boso peninsula shore (figure 5*a*). Since the fault trace undergoes a 40° bend near the tip of the Boso peninsula, the earthquake uplift is not recovered as a result of interseismic deformation (the relaxation of the lower crust) or slip on adjacent fault segments, and so a set of uplifted marine terraces preserves the prehistoric record of great earthquakes along the eastern Sagami trough (figure 5*b*). Greater Tokyo experienced a century of seismic quiescence after the 1703 earthquake (Okada 1994), and by analogy to the 1923 earthquake most faults north of fault A would have been inhibited from failure by the stress transferred by the 1703 event (figure 3*a*).
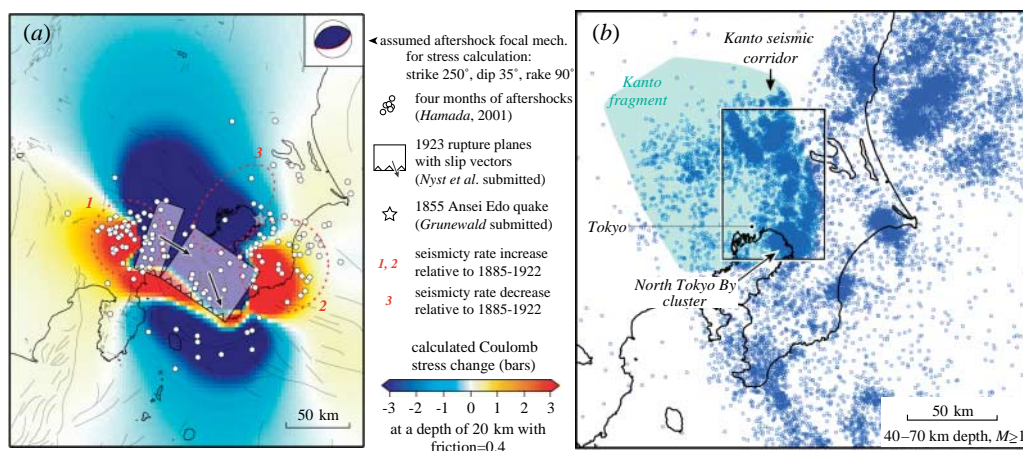
Figure 3. (*a*) Stresses imparted by the 1923 Kanto earthquake (Nyst *et al.* submitted) to the surrounding crust may explain the sites of increased and decreased seismicity (Hamada *et al.* 2001) for the ensuing decades. (*b*) Seismicity recorded during 1979–2004 in the Kanto region, revealing the concentration of earthquakes in the Kanto seismic corridor. The 23 July 2005 $M=6.0$ earthquake struck in the North Tokyo Bay cluster, a likely site for the 1855 $M\sim7.3$ Ansei-Edo event.

5. Historical earthquake magnitudes and locations

Following Bakun & Wentworth (1997), we use observed intensity distributions to estimate the magnitude, location, and approximate depth of historical earthquakes, as well as the covariance between location and magnitude. A set of 25 earthquakes with both intensity data and instrumental magnitudes, locations, and depths were used to develop a calibrated intensity attenuation relation (in other words, how shaking decays with earthquake size and with distance from the epicentre) for the Japanese archipelago (Bakun 2005). This relation was applied by Grunewald (submitted) to relocate earthquakes during the period 1600–1884 (figure 4). Some 15 shocks had sufficient intensity observations for stable solutions; analysis suggests that all $M\geq6.75$ shocks should be contained in our catalogue (figures 6*a* and 12).

6. Associating earthquakes with faults

The distribution and magnitude of deformation observed by GPS and geodetic levelling enabled Nishimura & Sagiya (submitted) to estimate the strain accumulation rate on the major faults, and thus to infer their seismic slip rates. The tectonic model introduced in figure 1 (Toda *et al.* submitted) supplied the fault locations and geometry. This analysis reveals that along the Suruga and Sagami troughs (sites of the 1854 $M=8.4$ Tokai, 1923 $M=7.9$ Kanto, and 1703 $M\sim8.2$ Genroku earthquakes), faults are locked and are thus accumulating strain to be released in future earthquakes (figure 7). In contrast, north of the Izu peninsula, the plate boundary faults partially creep and so produce earthquakes less frequently. Along the Japan Trench, the site of the 1938 $M\sim7.5$ earthquake swarm is locked, but the remainder of the Pacific subduction zone is creeping and
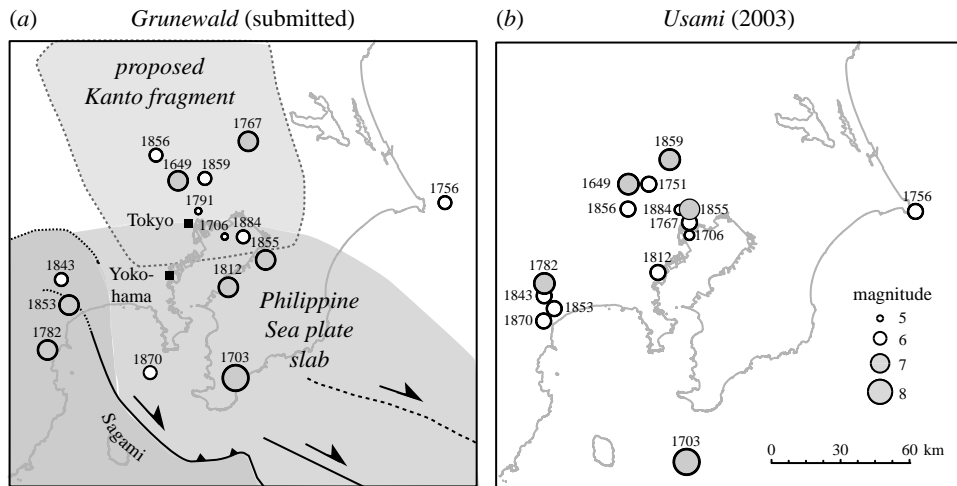
Figure 4. Map of the most probable locations of 1649–1884 earthquakes (Grunewald submitted) superimposed on our tectonic interpretation (Toda *et al.* submitted). The Philippine Sea plate is translucent, where it subducts beneath the Eurasian plate. In detail, each earthquake is represented by a probability density function for location with magnitude covariance, as shown in figure 12.

thus apparently has a low seismic potential. Overall, the inferred seismic slip rate is highest for the 1938 fault, intermediate for the faults on which the 1703, 1854 and 1923 earthquakes struck, and is poorly resolved for the presumed 1855 earthquake fault (figure 7).

The slip sustained in an earthquake, when divided by the fault slip rate, should correspond to the time between earthquakes (the inter-event time). Given the 6 m of oblique (right-lateral reverse) slip in the 1923 Kanto and 1703 Genroku earthquakes, and the inferred *ca* 25 mm yr^{-1} mean slip rate (figure 7), the mean inter-event time should be *ca* 250 years, considerably less than the *ca* 403±66 years (95% confidence) inter-event time observed from the marine terrace record (figure 5b). This disparity could mean that episodic or aseismic slip occurs on the fault that ruptured in 1923 and 1703, although GPS observations of such creep events are restricted to an area east of the Boso peninsula (Sagiya 2004).

7. The balance of seismic strain energy accumulation and release

Over a sufficiently long period, the rate of strain energy (or seismic moment) accumulation manifest in crustal deformation must balance the rate of seismic strain released in earthquakes. Nishimura & Sagiya (submitted) estimated the rate of seismic moment accumulation by the product of the fault areas and their slip rates from figure 7, multiplied by an assumed crustal stiffness (or elastic modulus). The earthquakes in the historical catalogue are represented by probability density functions for location and magnitude (figure 12). Through Monte Carlo simulation, Grunewald (submitted) estimated the most probable seismic moment release rate for AD 1649–2005 in the greater Kanto region from the catalogue. From this estimate, it is evident that the energy accumulation measured geodetically likely balances energy release represented by the
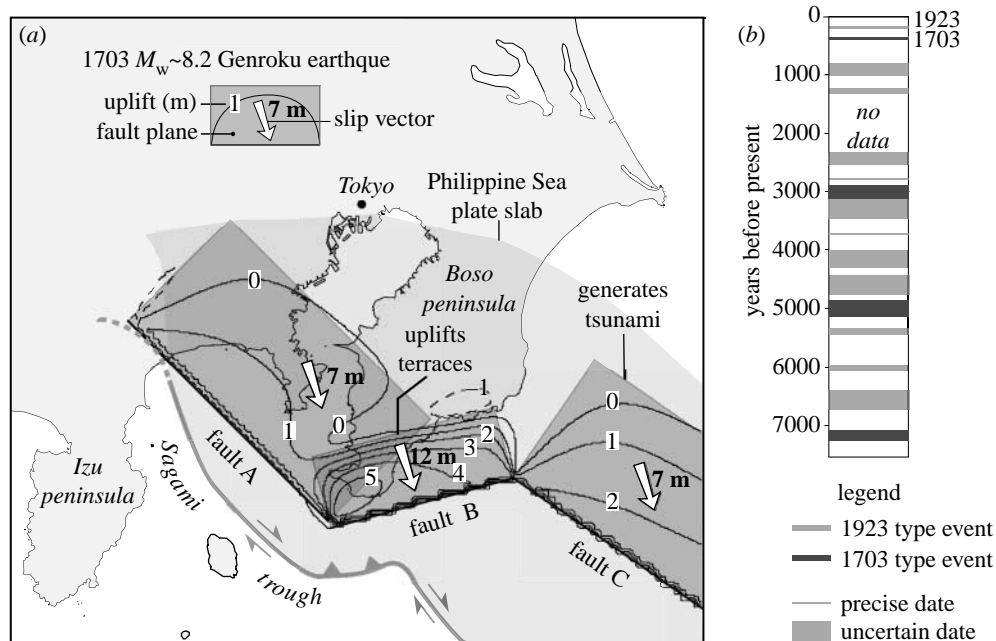
Figure 5. (*a*) Slip associated with the subduction of the Philippine Sea plate along the Sagami trough can explain the marine terrace uplift for Taisho (1923-type) and Genroku (1703-type) events, as well as the tsunami that accompanied the 1703 event (Shishikura *et al.* in preparation). (*b*) Observed marine terrace ages (Shishikura 2003). Event dates are shown in table 3.

earthquake catalogue, indicating that the catalogue is long enough to capture the range of seismic behaviour (figure 8). From this balance, we further infer that there is presently neither an earthquake deficit nor an earthquake over-abundance. This balance neglects permanent deformation, but since the quaternary coastal uplift is hundreds of metres and the cumulative fault slip is tens of kilometres, its influence is small and most energy is elastic.

8. Prehistoric record of great earthquakes

The Boso peninsula shoreline contains 16 marine terraces, each uplifted about 1.0–1.5 m during the past 7000 years and dated by Shishikura (2003; figure 5*b*). The southern tip of the Boso peninsula was uplifted 6.0 m in 1703 and 1.8 m in 1923. Although the 1703 Genroku shock was much larger than the 1923 Taisho earthquake, the inferred slip on the fault segment at the mouth of Tokyo bay is similar, *ca* 6–8 m (fault A in figure 5*a*); the 1703 earthquake also rupturing one or more segments to the east, resulting in greater Boso peninsula uplift. This suggests that each great Sagami trough earthquake permanently uplifts a marine terrace. Four of the southern Boso terraces were uplifted 4–6 m, and these resemble deformation that accompanied the 1703 $M{\sim}8.2$ Genroku earthquake (figure 5*a*). Thus, by treating all terrace uplift events in a single a time series, we are measuring the recurrence behaviour of the Tokyo bay fault A, which slipped in all of the $M{\geq}7.9$ shocks.
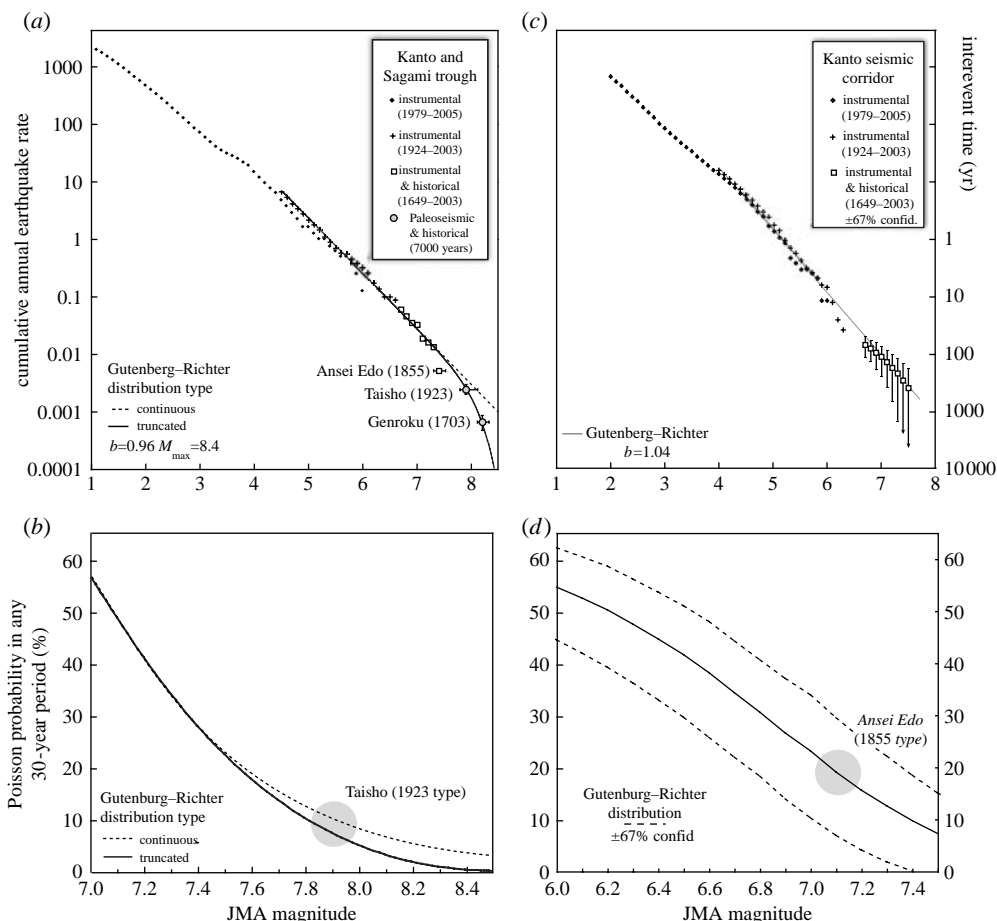
Figure 6. Magnitude–frequency distribution for relocated historical and instrumentally recorded $M \geq 4.5$ earthquakes in the Kanto region shown in figure 5. (*a*) A uniform, monotonic distribution with a *b*-value near 1.0. (*b*) Resulting time-averaged probability as a function of magnitude (Grunewald submitted). (*c*, *d*) Relationships for earthquakes within the Kanto seismic corridor (figure 3*b*).

9. Probability for $M \geq 7.9$ Kanto earthquakes

Large earthquake recurrence on a single fault is thought to be cyclic, and so the probability of the next earthquake depends on the time since the last one. When considering many faults in a region, the time-dependence of stress renewal on each individual fault is averaged out, and so a time-independent or Poisson probability may become appropriate. A Poisson probability can be regarded as a time-averaged estimate, rather than one in which the underlying process is random. In seismic hazard investigations, a further reason to employ a Poisson probability is that fewer assumptions are needed, and each assumption carries additional uncertainty. For the time-averaged probability (the likelihood of an earthquake during an *average* 30 year period), we require only the mean inter-event time and its uncertainty or aperiodicity for earthquakes of interest, such as the $M \sim 8$ 'Taisho' events on the
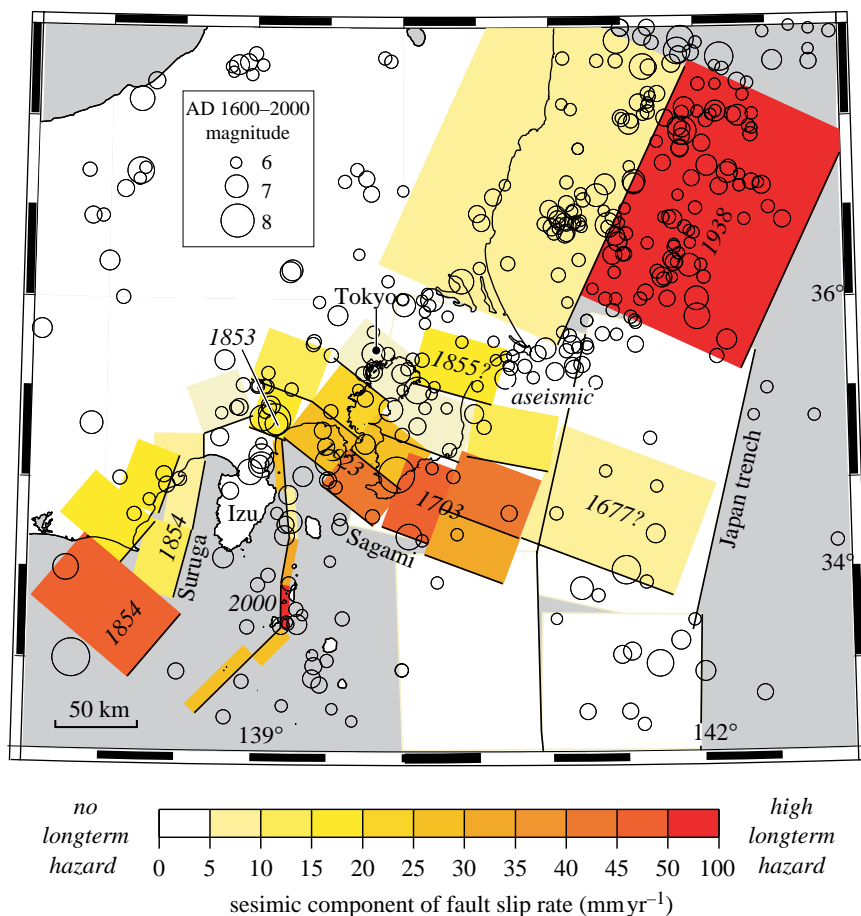
Figure 7. The inferred seismic slip rate (often called the 'slip deficit rate') for the major sources, and their association with larger historic events and historical seismicity, modified from Nishimura & Sagiya (submitted). Red sources slip at high rate and are presently locked, and thus are accumulating tectonic strain to be released in future large earthquakes; white sources have a low slip rate or creep, and so are unlikely to be sites of future large shocks.

Sagami fault. (Aperiodicity is 0 for perfectly regular recurrence, and 1 for perfectly random occurrence.) For time-dependent probabilities (the likelihood during the *next* 30 years), we use the time that has elapsed since, for example, the 1923 Taisho-type earthquake, and assume a probability density function to describe how the hazard grows with time since 1923. Required for both probability estimates are the dates of past events and the assumption that the fault slips approximately the same amount in each earthquake; the greater the number of dated earthquakes in the time series, the more useful the series becomes. Over many earthquake cycles, the Poisson probability will be the average of the renewal probabilities.

To estimate the Poisson probability of Taisho (1923 $M \geq 7.9$ type) earthquakes, we plot the frequency of all shocks within the Kanto area as a function of magnitude in figure 6a. This region includes the Sagami trough, but excludes the Suruga trough, because the $M \sim 8$ Tokai earthquakes there in 1707 and 1854 (figure 1) did not cause
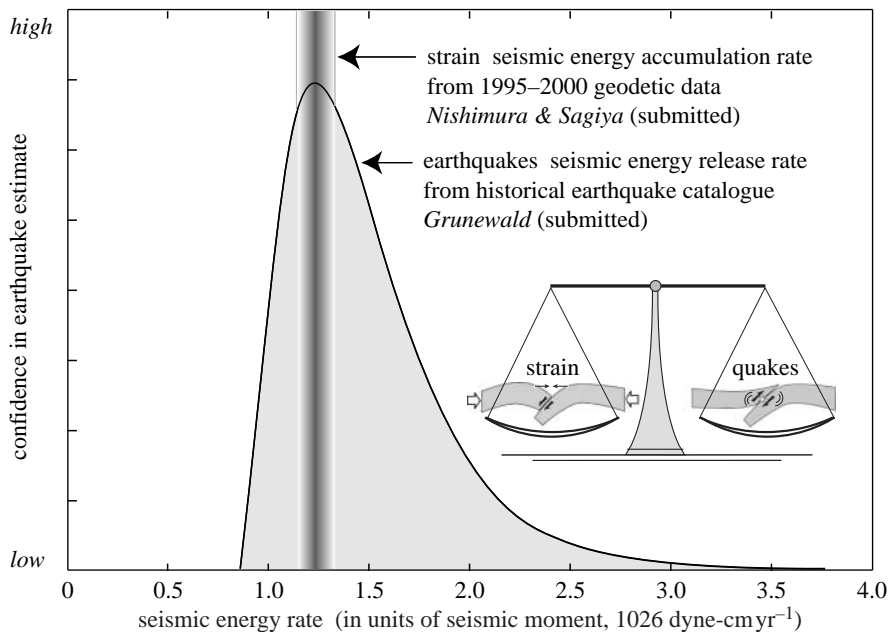
Figure 8. The agreement between the inferred rate of seismic moment release (Grunewald submitted) and seismic moment accumulation (Nishimura & Sagiya submitted) ensures that the catalogue reasonably represents the long-term seismic behaviour of the region. This also increases our confidence in the inferred seismic slip rates in figure 7.

JMA Intensity 6 shaking in Tokyo. We combine modern instrumental, historical and palaeoseismic data into one plot, which is fit by a Gutenberg–Richter relation for $4.5 < M \leq 8.2$. Whether the function is truncated depends on if the largest earthquakes are undersampled; both interpretations (the solid and dashed lines in figure 6a,b) are viable. Converting frequency, λ, into probability, p, by the relation $p = 1 - (\exp - \lambda N)$, where N is the time period (here, 30 years), we derive figure 6b. Thus for Taisho type ($M \geq 7.9$) earthquakes, the probability is 8–11% (figure 6b).

For the renewal probability, we use a new method, detailed in appendix A, to find the likely inter-event time and periodicity for 1923-type ('Taisho') events (figure 9). Remarkably, the resulting Taisho earthquake occurrence is more regular than for earthquakes of the same size and frequency on the San Andreas fault, where the aperiodicity is *ca* 0.8 (Weldon *et al.* 2004, 2005; Parsons 2005). Our renewal probability is more tightly constrained and slightly lower than that of the Japanese government; it is also well below the Poisson estimate, since we are presently only 20% into the mean earthquake cycle for $M \geq 7.9$ Taisho shocks (figure 9c).

10. Probability for $M \geq 7.1$ Ansei-Edo type earthquakes

Considering location and magnitude uncertainties, there have been six to seven $M \geq 7$ shocks within 50 km of Tokyo since 1649. Among the largest is the 1855 Ansei-Edo event, which produced JMA Intensity 6 shaking over much of the southern Kanto Plain (figure 2c). The Kanto seismic corridor (Toda *et al.* submitted)

presently contains the highest rate of Kanto seismicity (figure 3*b*), as well as most of the moderate historical earthquakes (figure 4*a*). Thus, we plot the frequency of all earthquakes within this corridor as a function of magnitude in figure 6*c*, which is well fit by a Gutenberg–Richter relation. We have no palaeoseismic record for Ansei-Edo events, since they are deep and leave little morphological evidence of their occurrence. We judge that most $M \geq 7.1$ shocks that fall within the corridor can produce JMA Intensity 6 shaking in Tokyo. The resulting probability is shown in figure 6*d*, yielding *ca* 20% in 30 years, although the confidence range in the historical catalogue is quite wide. The uncertainty would be much smaller if $4.0 \geq M \geq 7.5$ earthquake rates were fit in figure 6*b*. Details of this calculation are presented in appendix A.

Deducing a renewal probability for Ansei-Edo type events is hampered by several sources of uncertainty, but it is likely quite high. If, on the basis of their very similar intensity distributions, one assumes that the 1855 earthquake occurred at the location and 70 km depth of the 23 July 2005 earthquake (Grunewald submitted), then the 1855 earthquake resulted from thrust slip between the base of the Kanto fragment and the underlying Pacific plate. Velocity reconstructions by Toda *et al.* (submitted) give a slip rate of *ca* 55 mm yr^{-1} on this surface for the past 2 Myr. Based on the $7.2 \leq M \leq 7.5$ size of the 1855 earthquake and magnitude–slip scaling relationships from Wells & Coppersmith (1994), the mean slip would have been *ca* 3–8 m. This would yield a 50–150 years inter-event time. Even though the aperiodicity of this cycle cannot be assessed, we are now at or beyond the end of an earthquake cycle. Thus, the renewal probability would be much greater than the Poisson probability. A counter-argument is that only one earthquake of this size is evident in the 400 year historical record in the Kanto seismic corridor, so the inter-event time should be higher than our estimate. If the 1703 and 1923 shocks each inhibited the occurrence of Ansei-Edo shocks for 50–100 years (figure 3*a*); however, the historical record would be too short to be representative.

11. Combined earthquake probabilities

The combined time-averaged or Poisson 30 year probability for intensity ≥ 6 shaking is thus 29%, although the 67% confidence range on this estimate is wide (7–40%) because of the limitations of the historical catalogue. For the renewal probability, the likelihood of Ansei-Edo earthquakes is $\geq 35\%$, and for Taisho (1923-type) earthquakes, it is less than 1%, and so we can only suggest that the combined renewal probability is likely to be much higher than 35% (table 2). These probabilities correspond to the occurrence of JMA Intensity 6 shaking in greater Tokyo. Karim & Yamazaki (2002) used a set of earthquakes with intensity observations and strong ground motion data to deduce the ground acceleration and velocity values associated with the intensities (table 1), finding that JMA Intensity 6 corresponds to a peak horizontal ground acceleration (PGA) of 0.95*g* (0.7–1.5*g*) and a peak ground velocity of 0.93 m s^{-1} (0.5–1.0 m s^{-1}). Since intensities were historically measured in 1–2 storey wood or masonry buildings, they are principally sensitive to accelerations in the 5–8 Hz frequency range.
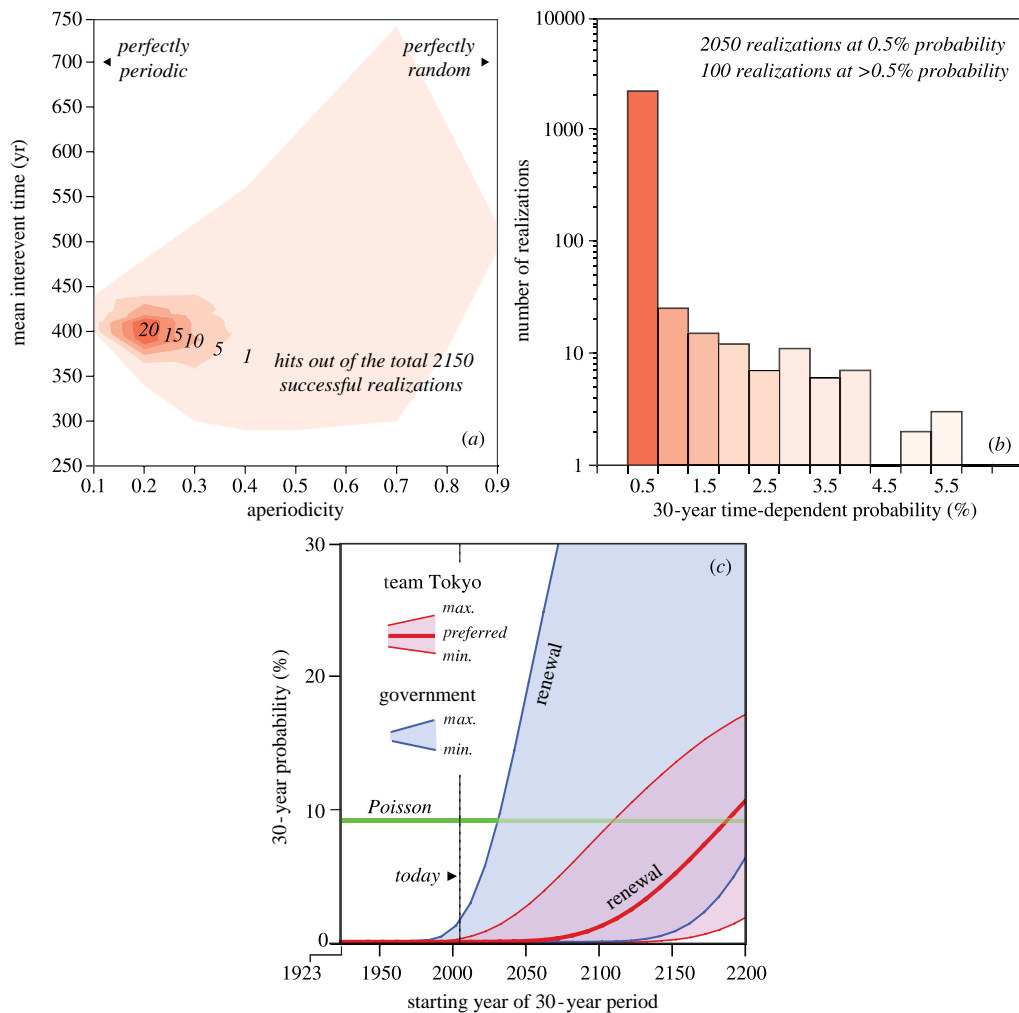
Figure 9. (*a*) Probability distribution for the mean inter-event time and aperiodicity for Taisho (1923-type) Sagami trough earthquakes. (*b*) Resulting time-dependent 30 year probability. (*c*) Our 30 year time-dependent (renewal) and time-averaged (Poisson) probabilities as a function of time, as well as the renewal probability for the government report, for which an inter-event time of 200–400 year and an aperiodicity of 0.17–0.24 were assumed (Earthquake Research Committee 2005).

12. Model corroboration by observed intensities

To corroborate our probability models, we constructed a time-averaged assessment exclusively from the observed intensities (Bozkurt *et al.* submitted). This method assumes only that the 400 year catalogue is representative of the long-term seismic behaviour, an assumption consistent with the balance between catalogue strain energy release and geodetically estimated energy accumulation (figure 8). For this assessment, we neither locate nor estimate the size of earthquakes, nor do we identify fault sources or their slip rates. Instead, we simply plot the frequency–intensity distribution for all 10 000 intensity

Table 2. Summary 30 year earthquake probabilities for greater Tokyo. (Note that the combined probability in the government study is equivalent to $I_{JMA} \geq 4$, shaking strong enough to awaken sleeping people, but not enough to damage buildings.)

	Poisson	renewal
team Tokyo study (this study)		
$M \geq 7.3$ within 50 km of Tokyo (1855 Ansei-Edo type)	20 (0–30)	>35
$M \geq 7.9$ within 100 km of Tokyo (Taisho or Genroku type)	11 (7–13)	0.5
combined probability (for $I_{JMA} \geq 6$ or PGA $\geq 0.9g$)	29 (7–40)	>35
government study (Earthquake Research Committee 2005)		
$M \geq 6.7$ within 80 km of Tokyo (1987 off-Chiba type)	70	—
$M \geq 7.9$ within 100 km of Tokyo (Taisho or Genroku type)	—	≤0.8
combined probability (for $I_{JMA} \geq 4$ or PGA ≥ 0.08–$0.10g$)	70	

observations, and fit the decay to an exponential relation (figure 10*a*). A power law satisfies the data nearly as well. The same exponent is then fit to the small number of observations that are typically available in each of 2000 5×5 km cells throughout Kanto (figure 10*b,c*), to produce a spatially variable probability map. The resulting probabilities (figure 11*a*) reveal a positive correlation with proximity to the major plate boundary faults, as well as with stream deposits and bay mud that amplify the shaking in unconsolidated sediments (figure 11*b*). The resulting probability of experiencing intensity ≥ 6 shaking is 37% in Tokyo, 34% in Yokohama and 11% in Chiba, in good agreement with our other estimate (table 2).

13. Human, structural and financial consequences of a large Tokyo earthquake

The Cabinet Office of the Japanese government recently issued a risk assessment for large Tokyo earthquakes (Central Disaster Management Council 2005). They considered an $M = 7.3$ earthquake beneath Tokyo, similar to the 1855 Ansei-Edo shock. The 240 000–840 000 destroyed buildings in their estimate depend strongly on wind speed and time of day, because high winds spread fire and rush hour exposes people to falling objects. If an $M = 7.3$ earthquake struck at 18.00 in 15 m s^{-1} (33 miles h^{-1}) winds, the Cabinet Office estimates 11 000 deaths, 210 000 wounded and 96 million tons of wreckage. About 57% of the deaths and 77% of the housing collapses are attributable to fire, and 28% of deaths and 18% of the collapses are due to shaking. The projected cost of an $M = 7.3$ earthquake beneath Tokyo are \$1.0 trillion (USD), which is 130% of the Japanese annual budget (Central Disaster Management Council 2005). Only about 5% of this loss is thought to be insured, and so the cost would be borne principally by home and business owners and the government. The total comprised \$587 million direct losses associated with recovery and rebuilding, and \$395 million in indirect losses due to production declines within and outside of Tokyo.
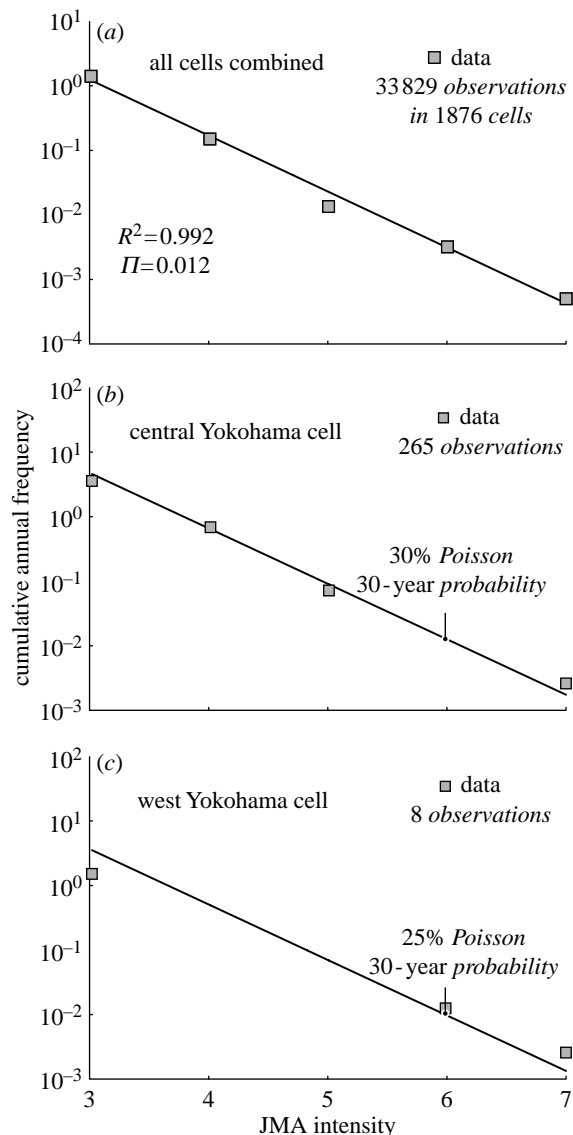
Figure 10. (*a*) The 10 000 intensity observations are collapsed onto one frequency–intensity distribution and fitted to an exponential decay curve. Modern data collected since the 1923 earthquake dominate the low-intensity observations, whereas data from 1600 to 1900 provide most of the high-intensity data. Fit of the general decay curve to sites in Yokohama with dense (*b*) and sparse (*c*) observations (Bozkurt *et al.* submitted) yield similar probability estimates.

Our 29% probability of an $M \sim 7.3$ Tokyo earthquake in 30 years corresponds to an annual probability of 1.2%. Thus, the annual probable loss for Tokyo is \$12 billion. Thus, in order to pay for the future earthquake, the Japanese government would need to save this amount annually, investing a portion to mitigate against future losses; but irrespective of Japanese actions, the consequences of a Tokyo earthquake of this magnitude are unlikely to be restricted to Japan. Japan is the

largest owner of US Treasury securities, holding \$700 billion or 17% of the total. How global capital markets would respond to a sudden withdrawal of these and other funds is unknown.

14. Conclusions

We have pursued several approaches to estimating the likelihood of severe earthquake shaking in greater Tokyo. The time-averaged and renewal earth-quake probabilities both tend to produce answers of about 30% likelihood of intensity≥6 shaking in the next 30 years. The weakness in our renewal probability is uncertainty on the inter-event time for 1855 Ansei-Edo type events; the weakness in our Poisson probability is that it may not reflect conditions that govern earthquake occurrence for the next 30 years; but the singular benefit of the Poisson probability is that it can be corroborated by the observed intensity data free of most modelling assumptions. Such confirmation is rare if not unprecedented in seismic hazard analysis, and so in our judgment makes our findings credible and the consequences sobering.

Appendix A

A.1 Time-dependent probability

The renewal probability p is calculated by integrating a probability density function $f(t)$

$$p(t \leq T \leq t + \Delta t) = \int_{t}^{t+\Delta t} f(t)\mathrm{d}t, \tag{A 1}$$

between t and $t+\Delta t$, where $f(t)$ can be any appropriate distribution with the property that probability grows with time after the last event. We use a Brownian passage time distribution (Matthews *et al.* 2002) to describe how the hazard grows with time

$$f(t, \mu, \alpha) = \sqrt{\frac{\mu}{2\pi\alpha^2 t^3}} \exp\left(-\frac{(t-\mu)^2}{2\mu\alpha^2 t}\right), \tag{A 2}$$

where μ is the mean inter-event time, and α is the aperiodicity of the distribution, which grows with inherent recurrence variability. Log-normal or Weibull distributions would yield similar results for periods starting in 2005.

We seek to find all recurrence and variability behaviour that can satisfy observations with a Brownian passage time distribution. Using a newly developed method (Parsons 2005) and the marine terrace record (figure 5*b* and
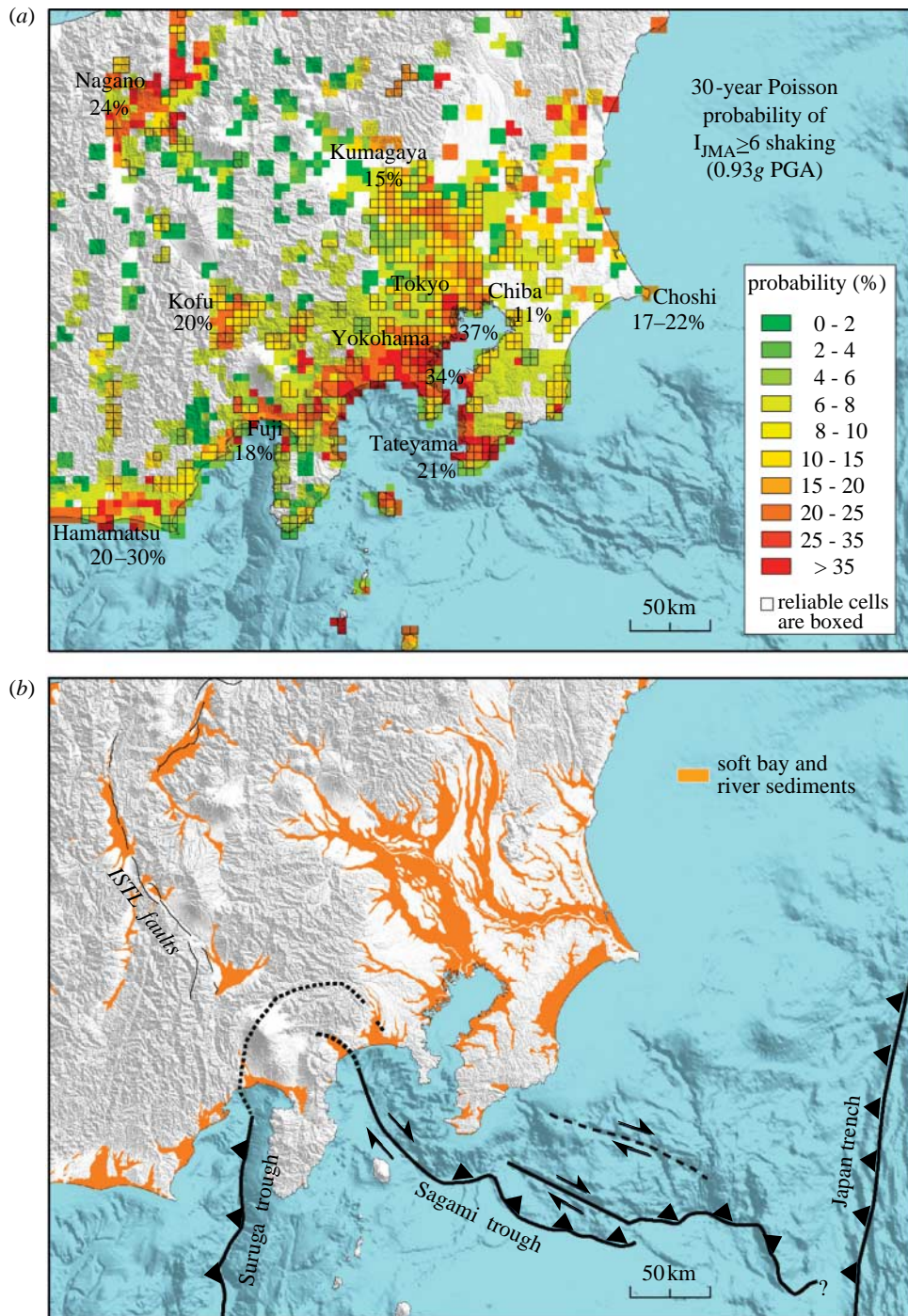
Figure 11. (*a*) Spatial distribution of the time-averaged 30 year probability of severe shaking (PGA ∼ 0.93*g*), which is consistent with our independent estimate (Bozkurt *et al.* submitted). (*b*) The probability of shaking is correlated with proximity to the plate-boundary faults and to sites of unconsolidated sediments. ISTL, Itoigawa-Shizuoka Tectonic Line.
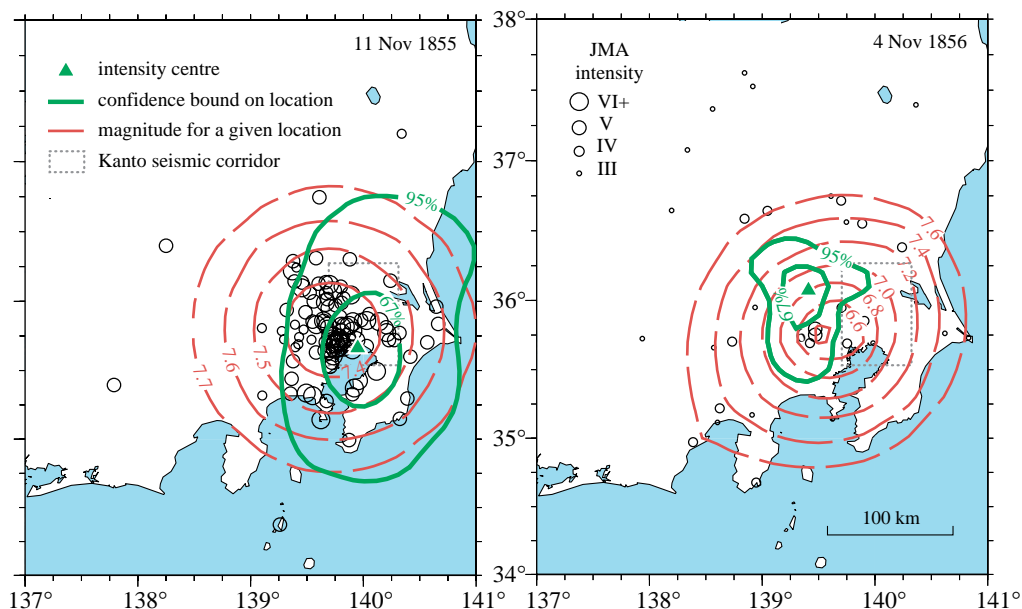
Figure 12. For each earthquake in our 1649–1885 catalogue of historic earthquakes (Grunewald submitted), there is a probability function on location (*green contours*) with covariance on magnitude (*red contours*), which arises because of data inadequacy and inconsistency (Bakun & Wentworth 1997). While the intensity centre for the 1856 earthquake corresponds to $M = 6.8$, the magnitude could range over $6.4 \geq M \geq 7.4$ depending on location. In the Monte Carlo sampling, the earthquake location is drawn 1000 times from a random sample consistent with the location function, and the associated magnitude is used in each case.

table 3), we constructed Brownian passage time distributions for all combinations of inter-event times from 250 to 750 years and aperiodicities from 0.1 to 0.9. For every pair of trial inter-event times and aperiodicities, we randomly drew a sequence of inter-event times in 5 million trials, starting with the oldest event, retaining the sequence only if all *ca* 17 events fell within the observed earthquake age ranges in table 3. The vast majority of such draws do not match the observations, but the distribution of the 2150 successful matches is contoured in figure 9*a*. The majority of the distributions fell within a narrow range: a mean inter-event time of 403 ± 66 years (95% confidence), with a mean 0.28 aperiodicity (0.2–0.4 at 92% confidence). The resulting 30 year probabilities for the likelihood of a $M \geq 7.9$ earthquake on the Sagami trough (fault A in figure 5) during the 30 year period, 2006–2035, range from 0 to 6%, with the dominant peak between 0 and 0.5% in 2005 (figure 9*b*).

A.2 Earthquake magnitude–frequency relation

We seek to assess the time-averaged (Poisson) likelihood of JMA Intensity 6 shaking in greater Tokyo. We thus plot the frequency of earthquakes as a function of magnitude for the Kanto region, which includes the Sagami but excludes the Sagami trough (figure 6*a*). We combine $M \geq 1.5$ earthquakes recorded since 1997, $M \geq 4.5$ earthquakes since 1924, $M \geq 6.7$ earthquakes since

Table 3. Kanto $M \geq 7.9$ earthquake record. (From Shishikura (2003), based on uplifted marine terraces (Nakata *et al.* 1980; Shishikura 2003) and tsunami deposits (Fujiwara & Kamataki 2003; Fujiwara *et al.* 1999). Historic earthquakes are assigned a ± 100 year range roughly equivalent to events dated by ^{14}C. Marine terraces were not formed during the period of rapid sea level rise, and so this time interval can contain any number of earthquakes, including none.)

event age range (calendar year)	earthquake evidence	number of earthquakes
AD 1823–2023	historic (1923)	1
AD 1603–1803	historic (1703)	1
AD 990–1220	dated terrace	1
AD 670–760	terrace	1
339 BC–AD 669	no data	any number
530–340 BC	dated terrace	1
889–650 BC	terrace and tsunami	1
1120–890 BC	dated terrace	1
1470–1121 BC	dated terrace	1
1870–1630 BC	dated terrace	1
2300–2000 BC	tsunami	1
2849–2301 BC	undated terrace	1
3050–2850 BC	terrace and tsunami	1
3450–3330 BC	terrace and tsunami	1
3949–3451 BC	undated terrace	1
4060–3950 BC	tsunami	1
4839–4161 BC	undated terrace	1
5020–4840 BC	terrace and tsunami	1

1649, and $M \geq 7.9$ earthquakes since 7500 years before present (from the marine terrace record) in one continuous curve in figure 6*b*. The 0.96 slope of the magnitude–frequency curve (called a '*b*-value') is typical of tectonic seismicity (where $0.9 \geq b \geq 1.1$), and the resulting frequency of $M \geq 7.9$ shocks can be transformed into a probability for a 30 year period of 9–11% (figure 6*c*) using $p = 1 - \exp(-\text{rate} \times \text{period})$.

Smaller earthquakes within the highly active Kanto seismic corridor (figure 3*b*), such as the 1855 Ansei-Edo shock, also produced JMA Intensity 6 shaking in Tokyo and Yokohama, so we plot a separate frequency–magnitude curve for this subset of the Kanto region. Whether a given earthquake falls within this smaller box is highly dependent on the location uncertainty. So, rather than use the intensity centre locations and their associated magnitudes shown in figure 4*a*, we created 1000 realizations of the catalogue by Monte Carlo simulation, drawing the earthquake locations according to the probability density functions. For example, it is evident in figure 12 that in *ca* 50% of the samples, the 1855 earthquake would fall within the Kanto seismic corridor, and in only 5% of the sampling would the 1856 earthquake lie within the corridor. Each earthquake location specifies a magnitude, and we further assume that the magnitude contours are uncertain by ± 0.1 magnitude units. We plot the mean and ± 1-sigma bounds on the frequency–magnitude relation for the 1000 realizations of the catalogue to capture the uncertainty inherent in the historical catalogue locations and

their covariance with magnitude. The resulting frequency curve is shown in figure 6*c* and the 30 year probability is shown in figure 6*d*. When these two probabilities are combined, the net probability for JMA Intensity 6 shaking in the greater Tokyo area is 29% (table 2).

References

Bakun, W. H. 2005 Magnitude and location of historical earthquakes in Japan and implications for the 1855 Ansei Edo earthquake. *J. Geophys. Res.* **110**, B02304. (doi:101029/2004JB003329)

Bakun, W. H. & Wentworth, M. C. 1997 Estimating earthquake location and magnitude from seismic intensity data. *Bull. Seismol. Soc. Am.* **87**, 1502–1521.

Bautista, B. C., Bautista, Ma. L. P., Stein, R. S., Barcelona, E. S., Punongbayan, R. S., Laguerta, E. P., Rasdas, A. R., Ambubuyog, G. & Amin, E. Q. 1996 Relationship of regional and local structures to Mount Pinatubo activity. In *Fire and mud: eruptions and lahars of Mount Pinatubo, Philippines* (ed. R. S. Punongbayan & C. G. Newhall), pp. 351–370. Qezon City, Philippines/Seattle, WA: Philippine Institute of Volcanology and Seismology/University of Washington Press.

Bozkurt, S., Stein, R. S. & Toda, S. Submitted. Forecasting probabilistic seismic shaking for greater Tokyo based on 400 years of intensity observations.

Central Disaster Management Council 2005 Report of the 15th special committee on the earthquake just beneath the Tokyo metropolis, 25 February, Cabinet Office, Government of Japan, Tokyo.

Earthquake Research Committee 2005 *Comprehensive study of probabilisitic seismic hazard map for Japan.* (2005). Tokyo, Japan: Headquarters for Earthquake Research Promotion. 125 pp.

Fujiwara, O. & Kamataki, T. 2003 Significance of sedimentological time-averaging for estimation of depositional age by ^{14}C dating on molluscan shells. *Quatern. Res. (Japan)* **42**, 27–40.

Fujiwara, O., Masuda, F., Sakai, T., Irizuki, T. & Fuse, K. 1999 Holocene tsunami deposits detected by drilling in drowned valley of the Boso and Miura Peninsulas. *Quatern. Res. (Japan)* **38**, 41–58.

Grunewald, E. Submitted. A new 1649–1884 catalog of destructive earthquakes near Tokyo and implications for the long-term seismic process.

Hamada, N., Kazumitsu, Y., Nishwaki, M. & Abe, M. 2001 A comprehensive study of aftershocks of the 1923 Kanto earthquake. *Bull. Seismol. Soc. Japan* **54**, 251–265.

Ishida, M. 1992 Geometry and relative motion of the Philippine Sea plate and Pacific plate beneath the Kanto-Tokai district, Japan. *J. Geophys. Res.* **97**, 489–513.

Ishida, M. 1995 The seismically quiescent boundary between the Philippine Sea plate and the Eurasian plate in central Japan. *Tectonophysics* **243**, 241–253. (doi:10.1016/0040-1951(94)00168-9)

Japan Meteorological Agency 2004 Annual Seismological Bulletin (CD-ROM), edited. Tokyo, Japan: JMA.

Karim, K. R. & Yamazaki, F. 2002 Correlation of JMA instrumental seismic intensity with strong motion parameters. *Earthquake Eng. Struct. Dyn.* **31**, 1191–1212. (doi:1110.1002/eqe.1158)

Matthews, M. V., Ellsworth, W. L. & Reasenberg, P. A. 2002 A Brownian model for recurrent earthquakes. *Bull. Seismol. Soc. Am.* **92**, 2233–2250. (doi:10.1785/0120010267)

Nakata, T. *et al.* 1980 Holocene marine terraces and seismic crustal movements in the southern part of Boso Peninsula, Kanto, Japan. *Geogr. Rev. Japan, Ser. A* **53**, 29–44.

National Museum of Japanese History 2003 Documenting disaster: natural disasters in Japanese history, 1703–2003, p. 167. Chiba, Japan: Foundation for Museums of Japanese History.

Nishimura, T. & Sagiya, T. Submitted. Crustal block kinematics around the northernmost Philippine Sea plate, central Japan estimated from GPS and leveling data.

Niu, F., Levander, A., Ham, S. & Obayashi, M. 2005 Mapping the subducting Pacific slab beneath southwest Japan with Hi-net receiver functions. *Earth Planet. Sci. Lett.* **239**, 9–17. (doi:10.1016/j.epsl.2005.1008.1009)

Noguchi, S. I. 1998 Seismicity, focal mechanisms and location of volcanic front associated with the subducting Philippine Sea and Pacific plates beneath the Kanto district, Japan. *Bull. Earthquake Res. Inst. Univ. Tokyo* **73**, 73–103.

Nostro, C., Stein, R. S., Cocco, M., Belardinelli, M. E. & Marzocchi, W. 1998 Two-way coupling between Vesuvius eruptions and southern Apennine earthquakes (Italy) by elastic stress transfer. *J. Geophys. Res.* **103**, 24 487–424 504. (doi:10.1029/98JB00902)

Nyst, M., Hamada, N., Pollitz, F. F. & Thatcher, W. Submitted. The stress triggering role of the 1923 Kanto earthquake.

Nyst, M., Nishimura, T., Pollitz, F. F. & Thatcher, W. In press. The 1923 Kanto earthquake re-evaluated using a newly augmented geodetic data set. *J. Geophys. Res.* (doi:10.1029/2005JB003628)

Okada, Y. 1994 Seismotectonics in the Tokyo metropolitan area, central Japan. *Proc. 9th joint meeting of the U.J.N.R. Panel on Earthquake Prediction Technology* **9**, 47–59.

Parsons, T. 2005 Significance of stress transfer in time-dependent earthquake probability calculations. *J. Geophys. Res.* **110**, B05S04. (doi:10.1029/2004JB003190)

Pollitz, F., Nyst, M. & Nishimura, T. 2005 Coseismic slip distribution of the 1923 Kanto earthquake, Japan. *J. Geophys. Res.* **110**, B11408. (doi:11410.11029/12005JB003638)

Pollitz, F., Nyst, N., Nishimura, T. & Thatcher, W. 2006 Inference of postseismic deformation mechanisms following the 1923 Kanto earthquake. *J. Geophys. Res.* **111**, B05408. (doi:10.1029/2005JB003901)

Sagiya, T. 2004 Interplate coupling in the Kanto district, central Japan, and the Boso silent earthquake in May 1996. *Pure Appl. Geophys.* **161**, 2601–2616. (doi:10.1007/s00024-004-2566-6)

Sato, H. *et al.* 2005 Earthquake source fault beneath Tokyo. *Science* **309**, 462–464. (doi:10.1126/science.1110489)

Shishikura, M. 2003 Cycle of interplate earthquakes along the Sagami Trough deduced from tectonic geomorphology. *Bull. Earthquake Res. Inst. Univ. Tokyo* **78**, 245–254.

Shishikura, M., Toda, S., & Satake, K. In preparation. Fault model of the 1703 Genoku Kanto earthquake (M 8.2) along the Sagami trough deduced from renewed coseismic crustal deformation.

Takemura, M. 2003 *The great Kanto earthquake, knowing ground shaking in greater Tokyo area.* Tokyo, Japan: Kajima Institute Publishing. 139 pp. [In Japanese.]

Toda, S. *et al.* Submitted. A slab fragment wedged under Tokyo: Consequences for earthquakes, volcanoes and geography.

Usami, T. 1994 *Seismic intensity maps and isoseismal maps of historical earthquakes of Japan.* Tokyo, Japan: Japan Electric Association.

Usami, T. 2003 *Materials for comprehensive list of destructive earthquakes in Japan [416]-2001*, p. 607. Tokyo, Japan: University of Tokyo Press.

Utsu, T. 1979 Seismicity of Japan from 1885 through 1925—a new catalog of earthquakes of $M \geq 6$ felt in Japan and smaller earthquakes which caused damage in Japan. *Bull. Earthquake Res. Inst. Univ. Tokyo* **54**, 253–308.

Utsu, T. 1982 Catalog of large earthquakes in the region of Japan from 1885 through 1980. *Bull. Earthquake Res. Inst. Univ. Tokyo* **57**, 401–463.

Weldon, R. J., Scharer, K. M., Funaml, T. E. & Biasi, G. P. 2004 Wrightwood and the earthquake cycle: what a long recurrence record tells us about how faults work. *GSA Today* **14**, 4–10. (doi:10.1130/1052-5173(2004)014<4:WATECW>2.0.CO;2)

Weldon, R. J., Fumal, T. E., Biasi, G. P. & Scharer, K. M. 2005 Past and future earthquakes on the San Andreas fault. *Science* **308**, 966–967. (doi:10.1126/science.1111707)

Wells, D. L. & Coppersmith, J. K. 1994 New empirical relationships among magnitude, rupture length, rupture width, rupture area, and surface displacement. *Bull. Seismol. Soc. Am.* **84**, 974–1002.

Discussion

R. BLONG (*Benfield, Australia*). What is the relationship between the 1703 Genroku earthquake and the 1707 Fuji eruption? If it was not fortuitous, why was not there an eruption after the 1923 earthquake? Will there be an eruption after the next great earthquake?

R. S. STEIN. These are fascinating questions that we hope to probe in a subsequent study.

The 31 December 1703 $M{\sim}8.2$ Genroku shock struck along the Sagami trough. Its western end lies just 40 km east of Mt Fuji. On 4–7 February 1704, sounds emanated from Mt Fuji that volcanologists today believe might indicate magma migration. Then, on 28 October 1707, the $M{\sim}8.6$ Tokai shock struck along the Suruga trough. Both great earthquakes occurred on the Philippine Sea plate slab. The nearest edges of the two great rupture surfaces were only about 80 km apart, and Mt Fuji lies between them. Some 49 days after the Tokai earthquake, the Hoei eruption of Mt Fuji began, one of the most violent in Fuji's 10 000 year history, with a tephra volume of 3 km^3 and a volcanic explosivity index of 5. This was the largest of the 30 or so eruptions of Fuji since 930 BC. There are reported to be frequent swarms of earthquakes beneath Fuji during the period between the Tokai earthquake and the Hoei eruption, although at least some of these are probably Tokai aftershocks. The 1923 Kanto earthquake caused no eruption of any kind, although some 1923 aftershocks also occurred at or near Mt Fuji (National Museum of Japanese History 2003).

We would like to study the earthquake and eruption time series more closely to see if they are correlated. Because great Tokai shocks recur roughly every 200 years and great Kanto shocks recur roughly every 400 years, few of these earthquakes can have triggered more than minor eruptive activity. We would also like to test whether Coulomb stresses imparted by the 1703 earthquakes might have compressed the magma chamber or opened magma conduits beneath Fuji, whether the 1703 shock promoted failure on the Suruga megathrust, and whether the Tokai earthquake, in turn, further compressed the magma chamber, triggering or hastening the eruption. We hypothesized such an interaction between the 1990 $M{=}7.8$ Luzon earthquake and the Mt Pinatubo eruption six months later (Bautista *et al.* 1996), and for the history of Apennine earthquakes and Vesuvius eruptions (Nostro *et al.* 1998).

S. SPARKS (*University of Bristol, UK*). How are the Japanese authorities responding to scientific information, and to the high probability of a Tokyo earthquake?

R. S. STEIN. This remains to be seen, but earthquakes are felt in Tokyo about once every two weeks, and these are probably the strongest public reminder of the looming risk. The Japanese government released its first-ever probabilistic earthquake hazard assessment in 2004, a departure from a historical focus on earthquake prediction. We regularly briefed the head of the government committee and members of his scientific team as we developed our findings, and they have generally been welcoming and receptive. Nevertheless, we have not approached any governmental authorities because we did not want to appear to be challenging the government committee. The Royal Society discussion

meeting was the first public presentation of our results, and we have yet to present a similar summary to the Japanese public.

H. Shah (*RMS and Stanford University, USA*). Since an insurance company supports your work, do you have plans to extend your work from seismic hazard to seismic risk for the Tokyo region?

R. S. Stein. Although we do not calculate the probability of the human or financial losses associated with a particular earthquake, we have added a brief discussion of the earthquake consequences based on Japanese research. We have also placed on our Team Tokyo web site an event set of the intensity distributions for the 15 largest earthquakes that have struck the greater Tokyo region during the past 400 years. Insurance companies and risk consulting companies can use these as scenario events to calculate losses to their insurance portfolios, building and lifeline inventories, or casualties.

J. Kennedy (*public attendee*). What is the distinction between earthquake prediction and forecasting?

R. S. Stein. Among earthquake researchers, 'prediction' is taken to mean an earthquake time, place and magnitude, with a high degree of specificity and reliability. This has not been achieved. A 'forecast' supplies the probability of these parameters over a given time period. The USGS issues reports containing 30 year forecasts, and has a web site that issues 24 h forecasts, http://pasadena. wr.usgs.gov/step/.